Trans. Phenom. Nano Micro Scales, 6(1): 13-26, Winter and Spring 2018
DOI: 10.7508/tpnms.2018.01.002

ORIGINAL RESEARCH PAPER

Flow field and heat transfer of Ag-MgO/water micropolar hybrid nanofluid in a permeable channel

Ghanbar. Ali. Sheikhzadeh, Mahdi. Mollamahdi*, Mahmoud. Abbaszadeh

Faculty of Mechanical Engineering, University of Kashan, Kashan, Iran

Received 17 February 2016; revised 22 January 2017; accepted 2 March 2017; available online 1 January 2018

ABSTRACT: In this study, the least square method is applied to study the laminar flow, heat transfer and microrotation of MgO-Ag/water micropolar hybrid nanofluid in a permeable channel. The bottom wall is hot and coolant fluid is injected into the channel from the top wall. The base fluid in the channel is water and volume fraction of nanoparticle (50% Ag and 50% MgO by volume) is between 0 and 0.02. By comparing the results which are obtained from Least Square Method (LSM) with those of obtained from numerical method (fourth order Rung-Kutta method), a good conformity can be seen between them. The effects of different parameters such as Reynolds number, volume fraction of nanoparticles and microrotation factor of nanoparticles on flow field and heat transfer are examined. The results show that by increasing Reynolds number, the temperature of the hybrid nanofluid reduces and the microrotation parameter near the hot wall decreases and near the permeable wall increases. Also, heat transfer increases, especially in high Reynolds numbers and volume fraction of nanoparticles, when the hybrid nanofluid are used instead of common nanofluid.

KEYWORDS: *Heat transfer; Least square method; Micropolar hybrid nanofluid*; *Permeable channel*

INTRODUCTION

Convection heat transfer has a great importance in many applications in engineering, technology and natural processes. One of these applications is cooling systems which are the main concerns of microelectronic industries. In most cases, heat transfer optimization of these systems is done by increasing their surface which increases the volume and size of these devices. To conquer this problem, new working fluid and effective cooling system are required. Nanofluids have been proposed as a new approach in this field. Nanofluids which have better thermal conductivity than common fluids are suspensions of nanoparticles with average sizes below 100 nm in a fluid such as water, oil and ethylene glycol. Nowadays, applications of nanofluids are studied in a wide range of researches and are used in medicine due to their enhancement properties than those of common fluids.

Various researches [1-12] have been conducted in the field of nanofluids which show that by adding nanoparticles to base fluid, heat transfer increases. The flow and heat transfer of naofluids in the channels is considered in recent years due to its importance in the industry. Binaco et al. [13] numerically investigated laminar forced convection flow of a Al_2O_3/water nanofluid in a circular tube. They showed that heat transfer increases when Reynolds number and volume fraction of nanoparticles increases.

Tahir and Mital [14] examined developing laminar forced convection flow of alumina/water nanofluid in a cir-cular tube subjected to a uniform wall heat flux. According to their results, the heat transfer coefficient linearly increases with both Reynolds number and volume fraction and non-linearley decreases with increasing the particle size.

Sheikholeslami et al. [15] studied laminar nanofluid flow in a semi-porous channel analytically in the presence of transverse magnetic field. They showed that by increasing the volume fraction of nanoparticles, heat transfer increases.

Although nanofluids individually have the above-mentioned advantages in many practical applications, in order to gain better properties and increase heat transfer in fluid flow, the hybrid nanofluids as a new group of nanofluids have been introduced that have more enhanced properties.

Hybrid nanofluids have better thermal conductivity, chemical stability, physical strength, mechanical resistance and so on than individual nanofluids. Different researches have been done and different experimental models of hybrid nanofluid have been introduced in recent years. Wang et al. [16] measured effective thermal conductivity of mixtures of fluids and nanoparticles.

They used Al_2O_3 and CuO as nanoparticles and water as a base fluid.

According to their results, the thermal conductivities of nanoparticle–fluid mixtures are higher than nanofluids. Selvakumar et al. [17] experimentally examined the effect of using Al_2O_3–Cu/water hybrid nanofluid in cooling of electronic components.

*Corresponding Author Email: *mahdimollamahdi@gmail.com*
Tel.: +989196635245; Note. This manuscript was submitted on *February* 17, 2016; approved on *January* 22, 2017; published *January* 1, 2018

Nomenclature

C	Species concentration	T	Temperature(K)
f	dimensionless stream function	u,v	Velocity components in *x* and *y* direction
g	dimensionless micro rotation	v_w	Velocity of cooling injection fluid
LSM	Least square method	*x*	Horizontal axes coordinate
NUM	Fourth order Rung-Kutta numerical method	*y*	Vertical axes coordinate
j	micro-inertia density		**Greek Symbols**
N	micro rotation/angular velocity	η	Similarity variable
a	Distance between parallel walls	α	Expansion ratio
$a(t)$	Expand or contract function	φ	Nanoparticle volume fraction
c_p	Specific heat at constant pressure (Jkg-1K-1)	θ	Dimensionless temperature
A_{1-4}	Constant parameters in nanofluids	ρ	Density(kgm^{-3})
k	Coefficient of thermal conductivity($Wm^{-1}K^{-1}$)	μ	dynamic viscosity
m	Temperature power index	ν	Kinematic viscosity
Nu	Nusselt number	κ	coupling coefficient
P	Pressure(Pa)	ψ	Stream function(m^2s^{-1})
Pr	Prandtl number	ϕ^*	Trial function
q	Micro rotation factor		**Subscripts**
R	Residual function	*f*	Fluid
Re	Reynolds number	*nf*	Nanofluid
		s	Solid

Their experimental results indicate that the convective heat transfer coefficient of the heat sink is increased considerably when hybrid nanofluid was applied as the working fluid instead of water. Suresh et al. [18] investigated laminar convective heat transfer through a uniformly heated circular tube using Al_2O_3–Cu/water hybrid nanofluid. They showed that a maximum enhancement of 13.56% in Nusselt number at a Reynolds number of 1730 occurs compared to Nusselt number of pure water. Their results illustrate that 0.1% Al_2O_3–Cu/water hybrid nanofluids have slightly higher friction factor than 0.1% Al_2O_3/water nanofluid. Hemmat et al. [19] found an experimental correlation for Ag–MgO/water hybrid nanofluid with the particle diameter of 40(MgO) and 25(Ag) nm and nanoparticle volume fraction range between 0% and 2%. Moghadassi et al. [20] numerically investigated the laminar forced convection heat transfer in a horizontal circular tube. They showed that for Al_2O_3–Cu/water hybrid nanofluids, the average Nusselt number increases 4.73% and 13.46% comparing to Al_2O_3-water and pure water, respectively.

The theory of micropolar fluid was introduced by Eringen [21]. There are two kinematic vector fields in this theory: general velocity field and axis of the rotation vector which shows the spin movement or micro rotation of the rigid particles of micropolar fluid. The theory is made up of a new transport equation for micro rotation with some material parameters. Bourantas and Loukopoulos [22] studied theoretically differentially heated natural convection of micropolar nanofluid of Al_2O_3-water in a cavity. They showed that the microrotation of nanoparticles in suspension decreases overall heat transfer. Hussain et al. [23] investigated theoretically micropolar nanofluid flow over a stretching surface. According to their results, microrotation has decreasing influence on the skin friction and increasing effect on the heat transfer rate of the nanofluid. Ahmed et al. [24] studied numerically the laminar mixed convection flow in a square lid-driven enclosure filled with water-based micropolar nanofluid by using the finite volume method. Based on their results, the average Nusselt number increases when the solid volume fraction increases. The other researches which are dedicated to the use of micropolar fluid and nanofluid in convective heat transfer problems are presented in [25-30]. According to the reviewed available researches, it is observed that no study was done in the field of using micropolar hybrid nanofluid in channels.

When the analytical solution of a problem is impossible or very difficult, analytical-approximate methods such as the weighted residuals methods are used. The most popular of these methods is the Least Square Method (LSM). Initial works were performed by these methods in various cases. Stern and Rasmussen [31] solved a third order linear differential equation using collocation method. Vaferi et al. [32] investigated the possibility of using the orthogonal collocation method to solve diffusivity equations in the radial transient flow system. Recently the least square method have been used by Aziz and Bouaziz [33] to prognosticate the performance of the longitudinal fins. They found that the least square method is simpler than

other analytical methods. Sheikholeslami et al. [34] studied laminar flow of nanofluids in a semi-porous channel in the presence of a magnetic field by use of the Galerkin and least square methods. They found that by decreasing Reynolds number and increasing Hartmann number, the thickness of the velocity boundary layer increases. Hatami et al. [35] examined nanofluid flow and heat transfer in an asymmetric porous channel with expanding or contracting wall. They used the least square method and Galerkin method to simulate the problem. They illustrated that the Nusselt number increases with an increase of the nanoparticle volume fraction and Reynolds number. Hatami et al. [36] employed the least square method and numerical method to analyze the flow and heat transfer of nanofluid between contracting rotating disks. Their results indicate that as the wall permeability parameter increases, temperature increases and the position of maximum radial velocity is shifted towards the middle of two disks.

According to the above survey, it is illustrated that several investigations have been performed in the field of using nanofluid in channels, but using the hybrid nanofluid in channels does not receive any attention in last decade. So in this study, the laminar flow of a micropolar hybrid nanofluid in a channel with permeable wall is examined using the least square method. The conformity of the results of the least square analytical-approximate method with Rung-Kutta numerical method is checked and the effect of the Reynolds number, volume fraction of nanoparticles, expanding ratio and microrotation on heat transfer are considered. Also Nusselt number of hybrid nanofluid is compared with common nanofluid.

THE GOVERNING EQUATIONS AND BOUNDARY CONDITIONS

In this problem, the laminar flow of micropolar hybrid nanofluid in a permeable channel is investigated. The geometry of the problem is shown in Figure 1.

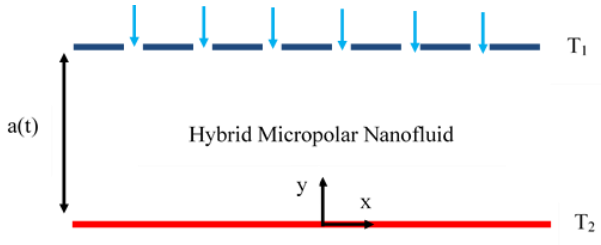

Fig. 1. Geometry of the problem

The bottom wall is hot and is cooled by a micropolar hybrid nanofluid which is injected into the channel with velocity v_w from the permeable top wall. The distance between the two walls is a(t) and the *x*-axis is coincided to the bottom wall. The temperature of the bottom wall is T_2 and the top wall temperature is T_1. Thermo-physical properties of water as the base fluid and Ag and MgO nanoparticles are presented in Table 1. Thermo-physical properties of water as the base fluid and Ag and MgO nanoparticles are presented in Table 1.

Table 1
Thermophysical properties of base fluid and nanoparticles [35, 37].

	ρ(kg/m^3)	c_p (j/kg K)	K (W/ m K)	Pr
MgO	3560	955	45	-
Ag	10500	235	429	-
Pure Water	997.1	4179	0.613	6.2

The diameter of MgO and Ag nanoparticles are 40 and 25nm respectively. The range of nanoparticles volume fraction (50% Ag and 50% MgO by volume) is between 0% and 2%.

The density and heat capacity of hybrid nanofluid are obtained from mixture relations 1 and 2 [38-39]. These relations are usually used for common nanofluids, but several studies have been used from them for hybrid nanofluids [40-43].

Also the viscosity and thermal conductivity are obtained from relations 3 and 4 according to experimental results presented by Hemmat et al [19]. The viscosity and thermal conductivity of Mg-Ag/water are showed at Figure 2.

$$\rho_{nf} = (1-\varphi)\rho_f + \varphi\rho_s \tag{1}$$

$$\rho_{nf} c_{p_{nf}} = (1-\varphi)c_{p_f}\rho_f + \varphi c_{p_s}\rho_s \tag{2}$$

$$\frac{\mu_{nf}}{\mu_f} = 1 - 32.795\varphi - 7214\varphi^2 + 714600\varphi^3 - 0.1941\times 10^8\varphi^4 \tag{3}$$

$$\frac{k_{nf}}{k_f} = \frac{0.1747\times 10^5 + \varphi}{0.1747\times 10^5 - 0.1498\times 10^6\varphi + 0.1117\times 10^7\varphi^2 + 0.1997\times 10^8\varphi^3} \tag{4}$$

In order to calculate the thermal conductivity and viscosity of MgO/water nanofluid, one time the Maxwell [44] and Brinkman [45] model has been used and another time, Corcione [46] model has been applied. The Maxwell and Brinkman relations are as follows:

$$\frac{\mu_{nf}}{\mu_f} = \frac{1}{(1-\varphi)^{2.5}} \tag{5}$$

$$\frac{k_{nf}}{k_f} = \frac{2k_s + k_f + \varphi(k_s - k_f)}{2k_s + k_f - 2\varphi(k_s - k_f)} \tag{6}$$

Corcione relations for calculating the thermal conductivity and viscosity of MgO/water nanofluid are presented at 7 and 8. It is worth mentioning that the

nanoparticles diameter is 40 nm, the diameter of water particles is 0.385 nm, and the average temperature is considered 24.7ºC [19].

The viscosity and thermal conductivity of Mg/water nanofluid are showed at Figure 2 based on Maxwell and Brinkman and Corcione model.

$$\frac{\mu_{nf}}{\mu_f}=\frac{1}{1-34.87\left(\frac{d_s}{d_f}\right)^{-0.3}\varphi^{1.03}} \tag{7}$$

$$\frac{k_{nf}}{k_f}=1+4.4\,\mathrm{Re}^{0.4}\,\mathrm{Pr}^{0.66}\left(\frac{T}{T_{fr}}\right)^{10}\varphi^{0.66} \tag{8}$$

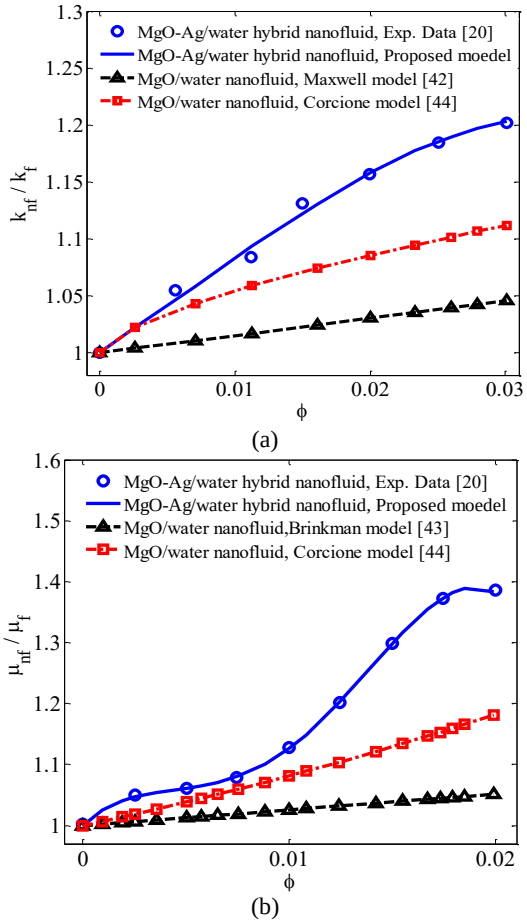

Fig. 2. Curve fitting on experimental Data of hybrid nanofluid [20] and theorical models for a) Conductivity, and b) Viscosity

The Reynolds and Prandtl numbers in relation 8 are obtained with the aim of relations 9 and 10.

$$\mathrm{Pr}=\frac{\mu_f}{\rho_f\,\alpha_f} \tag{9}$$

$$\mathrm{Re}=\frac{2\rho_f K_B T}{\pi\,\mu_f^2\,d_s} \tag{10}$$

The governing equations of the problem are [47]:

$$\frac{\partial u}{\partial x}+\frac{\partial v}{\partial y}=0 \tag{11}$$

$$\rho_{\mathrm{nf}}\left(\frac{\partial u}{\partial t}+u\frac{\partial u}{\partial x}+v\frac{\partial u}{\partial y}\right)=-\frac{\partial P}{\partial x}+\left(\mu_{\mathrm{nf}}+\kappa\right)\left[\frac{\partial^2 u}{\partial x^2}+\frac{\partial^2 u}{\partial y^2}\right]+\kappa\frac{\partial N}{\partial y} \tag{12}$$

$$\rho_{\mathrm{nf}}\left(\frac{\partial v}{\partial t}+u\frac{\partial v}{\partial x}+v\frac{\partial v}{\partial y}\right)=-\frac{\partial P}{\partial y}+\left(\mu_{\mathrm{nf}}+\kappa\right)\left[\frac{\partial^2 v}{\partial x^2}+\frac{\partial^2 v}{\partial y^2}\right]-\kappa\frac{\partial N}{\partial x} \tag{13}$$

$$\rho_{\mathrm{nf}}\left(\frac{\partial N}{\partial t}+u\frac{\partial N}{\partial x}+v\frac{\partial N}{\partial y}\right)=-\frac{\kappa}{j}+\left(2N+\frac{\partial u}{\partial y}-\frac{\partial v}{\partial x}\right)+\left(\mu_{\mathrm{f}}+\frac{\kappa}{2}\right)\left[\frac{\partial^2 N}{\partial x^2}+\frac{\partial^2 N}{\partial y^2}\right] \tag{14}$$

$$\rho_{\mathrm{nf}}\left(\frac{\partial T}{\partial t}+u\frac{\partial T}{\partial x}+v\frac{\partial T}{\partial y}\right)=\frac{k_{nf}}{c_{p_{nf}}}\frac{\partial^2 T}{\partial y^2} \tag{15}$$

in which u and v are the velocity components in the x and y directions, respectively.

ρ is the fluid density, μ is the dynamic viscosity, c_p is specific heat at constant pressure, j is the micro rotation viscosity, k is the vortex viscosity, k is the thermal conductivity, and N is micro rotation velocity. The boundary conditions of the problem can be expressed as follow:

$$u=0,\ v=0,\ T=T_1,\ N=-S\frac{\partial U}{\partial Y}=0 \quad \text{at y=0} \tag{16}$$

$$u=0,\ v=-v_w,\ T=T_1,\ N=-S\frac{\partial U}{\partial Y}=0 \quad \text{at y=a(t)} \tag{17}$$

N=0 represents that the microelements which are near to the wall are impotent to rotate. The temperature of the fluid at a η distance from the wall and the temperature of the heated wall are defined as follows:

$$T=T_1+\sum C_m\left(x/a\right)^m\theta_m\left(\eta\right) \tag{18}$$

With boundary conditions:

$$\theta_m(0)=1, \qquad \theta_m(1)=0 \tag{19}$$

When the wall temperature is expressed as a polynomial variation (equation 18), calculating a single value for the heat transfer coefficient along the hot wall is not conceivable. Therefore, the hot wall temperature should be considered as:

$$T_2 = T_1 + \sum C_m (x/a)^m \theta_m(0) \tag{20}$$

The similarity parameters are given by:

$$u = -\frac{\nu}{a^2} x F_\eta(\eta,t), \quad v = \frac{\nu}{a} F_\eta(\eta,t), \quad N = \frac{\nu}{a^2} x G(\eta,t), \quad \eta = \frac{y}{a(t)} \tag{21}$$

When the above parameters are put in equations 11 to 15, these equations change as follows:

$$(1+A_1 q)\left(\frac{A_2}{A_1}\right) f^{(4)} - qA_2 g'' + 3\alpha f'' + \alpha\eta f''' + \left(f' f'' - f f'''\right)\mathrm{Re} = 0 \tag{22}$$

$$(1+\frac{q}{2}A_1)\left(\frac{A_2}{A_1}\right) g'' + \alpha\xi\left(3g + \eta g'\right) + \mathrm{Re}\,\xi f' g - \mathrm{Re}\,\xi f g' - qA_1\left(\frac{A_2}{A_1}\right)\left(2g - f''\right) = 0 \tag{23}$$

$$\theta'' = \mathrm{Pr}\left(\frac{A_3}{A_4}\right)(-\alpha)\left(m\theta_m + \eta\theta'\right) - \mathrm{Pr}\left(\frac{A_3}{A_4}\right)\mathrm{Re}\left(mf'\theta + f\,\theta_m'\right) \tag{24}$$

Where $q = {}^{k}/_{\mu_f}$, $\xi = {}^{j}/_{a^2}$, $\alpha = a\dot{a}/\nu_f$ is the expansion ratio and it is positive when we have expansion and negative when we have contraction and m is the temperature power index. The other parameters are as follows:

$$A_1 = \frac{\mu_f}{\mu_{nf}}, A_2 = \frac{\rho_f}{\rho_{nf}}, A_3 = \frac{k_f}{k_{nf}}, A_4 = \frac{(\rho c_p)_f}{(\rho c_p)_{nf}} \tag{25}$$

$$f = \frac{F}{\mathrm{Re}}, \quad g = \frac{G}{\mathrm{Re}}, \quad \mathrm{Re} = \frac{v_w}{v_f} \tag{26}$$

It is noteworthy to say that the Reynolds number is positive for suction and negative for injection.
The boundary conditions are given by:

$$\theta(1)=0, \; f(1)=1, \; f'(1)=0, \; g(1)=0 \tag{27}$$

$$\theta(0)=1, \; f(0)=0, f'(0)=0, \; g(0)=0 \tag{28}$$

In this case the non-dimensional Nusselt number is obtained as:

$$Nu = -\frac{1}{A_3}\frac{\partial T}{\partial \eta}\Big/(T_2 - T_1) = -\frac{1}{A_3}\theta_m''(0) \tag{29}$$

METHODS

Analysis of the Least Square Method

One of the approximation techniques for solving differential equations is the Weighted Residual Methods (WRMs).

The weighted residual methods are general and tremendous powerful methods for obtaining approximate solutions for Ordinary Differential Equations (ODEs) or Partial Differential Equations (PDEs).

$$L_m(\phi) = f \quad \text{at } \Omega \tag{30}$$

where Lm denotes the differential operator with the highest order of derivative m in the Ω domain. Φ is the unknown function and f is a given function. The aim of solution is to seek a solution of Φ which satisfies equation 30.

Assume that Φ is approximated by a function Φ^* (trail solution), which is a linear combination of basic functions chosen from a linearly autonomous set. That is,

$$\phi \cong \phi^* = \sum_{i=1}^{n} c_i \varphi_i \tag{31}$$

By substituting equation 31 into 30, the result of the operations generally isn't f. It results in the so-called residual R, defined as:

$$R = L_m(\phi^*) - f \tag{32}$$

We can use some techniques to properly obtain an approximate function so as to make the residual as "small" as possible; we force the residual to zero in an average sense by setting weighted integrals of residuals to zero. For example, we impose

$$\int_{\Omega} RW_i d\Omega = 0 \quad i = 1,2,3,\cdots,n \tag{33}$$

Note that in WRMs, the number of weight functions W_i always equals the number of unknown constants c_i in ϕ^*. This yields n algebraic equations for the unknown constants c_i. In the LSM method, the summation of all the square of the residues should be minimized.

$$\zeta = \int_{\Omega} R^2 d\Omega = \sum_{i=1}^{n} \int_{\Omega_i} R_i^2 d\Omega = \sum_{i=1}^{n} \int_{\Omega_i} \left[L_m\left(\phi_i^*\right) - f_i \right] d\Omega \tag{34}$$

In order to achieve a minimum of the functional ζ, the derivatives of ζ with respect to all the unknown parameters must be zero. That is,

$$\frac{\partial \zeta}{\partial c_i} = 2\int_{\Omega} R \frac{\partial R}{\partial c_i} d\Omega = 0 \tag{35}$$

Comparing with equation 33, the weight functions are obtained. (Due to its value should be zero so we do not consider its constant.)

$$W_i = \frac{\partial R}{\partial c_i} \tag{36}$$

In order to use the least square method in this problem, the considered functions must be satisfied the boundary conditions of the problem. These functions are considered as equation 37 to 40 generally.

$$f = y^2 + c_1(y^2 - y^3) + c_2(y^2 - y^4) + c_3(y^2 - y^5) + c_4(y^2 - y^6) + c_5(y^2 - y^7) \tag{37}$$

$$f' = 2y + c_1(2y - 3y^2) + c_2(2y - 4y^3) + c_3(2y - 5y^4) + c_4(2y - 6y^5) + c_5(2y - 7y^6) \tag{38}$$

$$g = c_6(y - y^2) + c_7(y - y^3) + c_8(y - y^4) + c_9(y - y^5) \tag{39}$$

$$q = 1 - y + c_{10}(y - y^2) + c_{11}(y - y^3) + c_{12}(y - y^4) + c_{13}(y - y^5) \tag{40}$$

By introducing these equations into equations 17 to 19 the residual function is obtained and by substituting the residual functions into equations 32 to 35, a set of equations will obtain and by solving these algebraic equations, coefficients c_1–c_{13} will be determined.

Numerical solution

The numerical solution of the governing equations of the problem is the fourth order Runge-Kutta-Fehlberg method. This method is used for problems with definite boundary conditions.

In this method, the equations are solved for two time steps of h and h/2, and the results of the larger time step are compared with the smaller ones until the problem reach to the considered accuracy. This method is employed to solve various engineering and mathematical equations [48]. Also the convergence criterion in numerical simulation has been considered 10^{-5}.

RESULTS AND DISCUSSION

In this study, flow field and heat transfer and microrotation of MgO-Ag/water micropolar hybrid nanofluid are investigated in a channel with permeable and contracting or expanding wall using LSM analytical method and fourth order Rung-Kutta-Fehlberg numerical method. The effect of using the hybrid nanofluid is compared to common nanofluid.

Also the effects of parameters such as Re, φ, q and α on the flow filed and heat transfer are examined. The study is done for Re=1, 2 and 3, α=-1,0 and 1, q=0.2, 0.4 and 0.6, $\varphi = 0.00$ to 0.02, Pr=6.2, m=4 and $\xi = 1$.

Comparison of LSM and NUM

In Figure 3, the components of velocity(axial velocity, f and normal velocity, f'), temperature(θ) and micro rotation(g) which obtained from LSM are compared to those of NUM method for φ=0.02, q=0.2, Re=1 and α=-1. As can be seen from this figure, there is an excellent conformity between the LSM and NUM results. The conformity of the obtained temperature by using the LSM and NUM methods is less than the conformity of velocity components because of the temperature profile is considered by default.

Study of the effective parameters on flow and temperature field

In Figure 4, the effect of Reynolds number on axial and normal velocity profiles are shown for φ=0.02, q=0.2 and α=-1. As can be seen in this figure, by increasing Reynolds number the axial velocity component increases.

The normal velocity component has different behavior with changing Reynolds number so that for η< 0.5, with increasing of Re the f'component increases and for η> 0.5, with an increase of Re the f'component decreases. In Figure 5, the effect of Reynolds number on temperature is

shown at φ=0.02, *q*=0.2 and α=-1. Based on this Figure, by increasing Reynolds number the temperature of the hybrid nanofluid decreases.

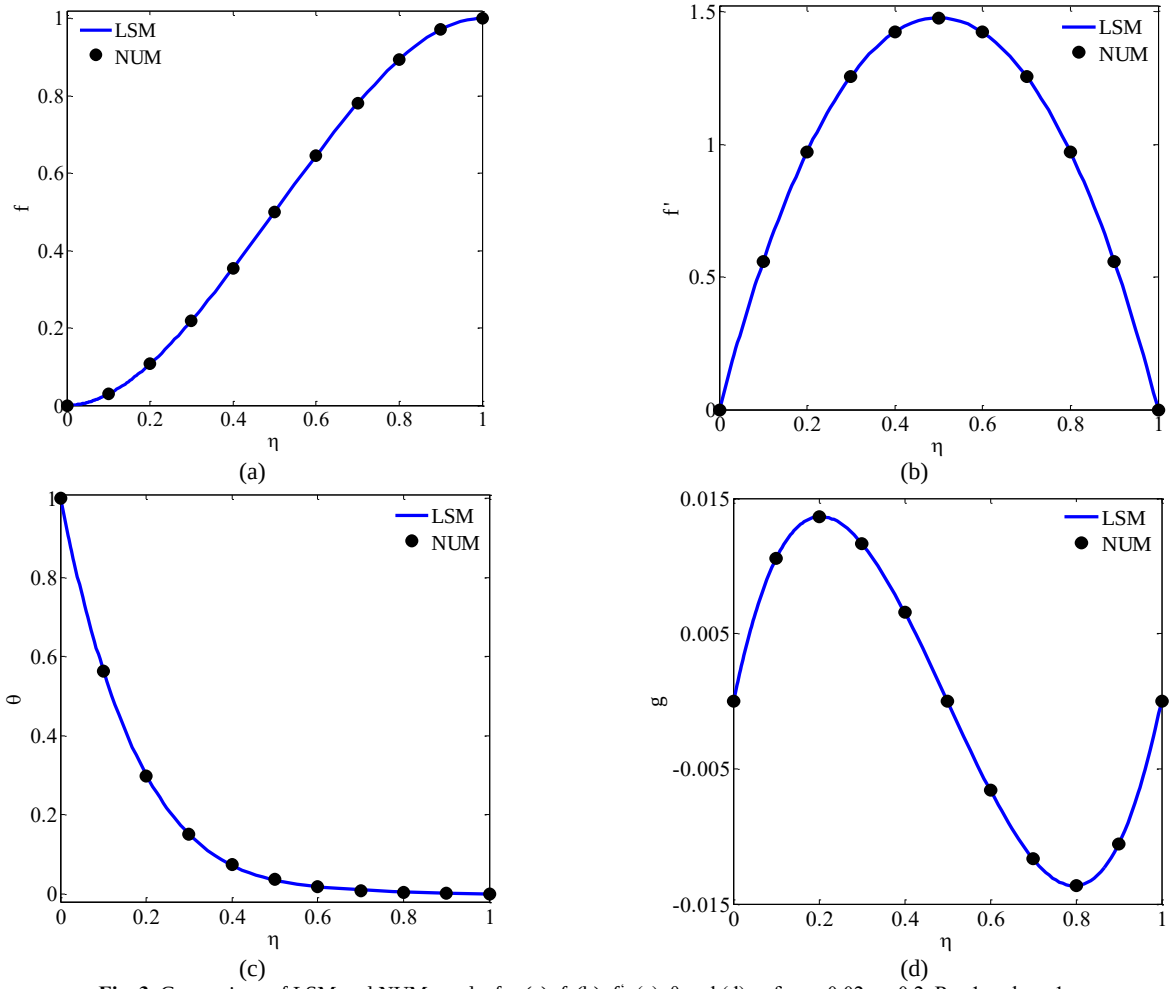

Fig. 3. Comparison of LSM and NUM results for (a). *f*, (b). *f*ˋ, (c). θ and (d). g for φ=0.02, q=0.2, Re=1 and α=-1

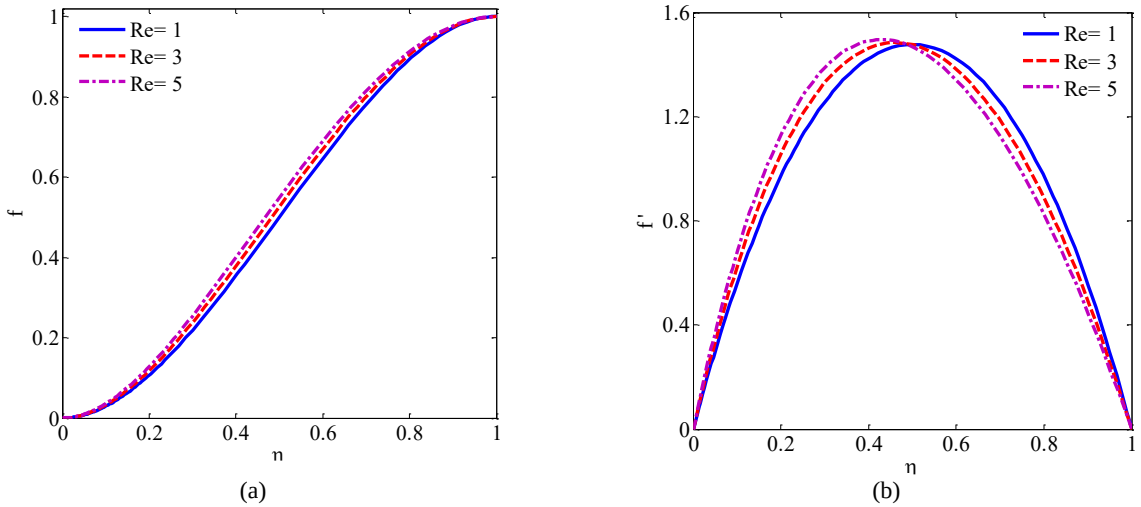

Fig. 4. Effect of Reynolds number on (a). f and (b). c for φ=0.02, q=0.2 and α=-1.

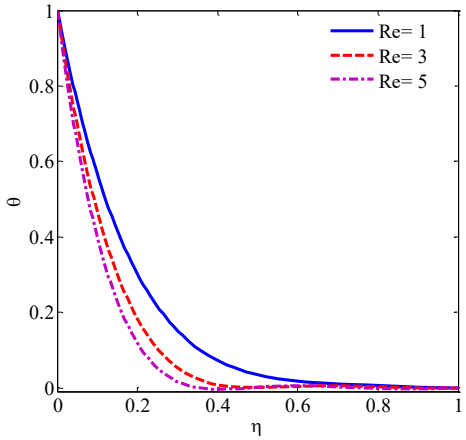

Fig. 5. Effect of Reynolds number on θ when φ=0.02, q=0.2 and α=-1

Also in figure 6, the variation of microrotation parameter in terms of η in different Reynolds numbers is illustrated

.

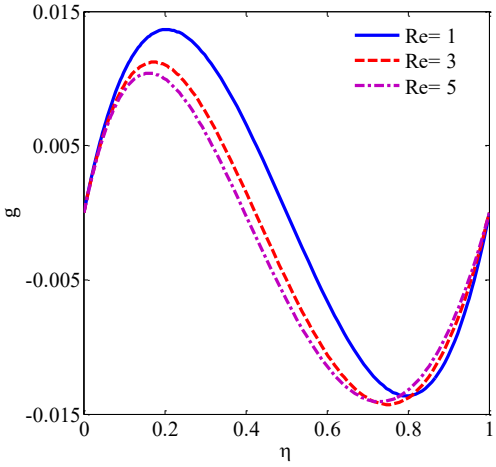

Fig. 6. Effect of Reynolds number on g when φ=0.02, q=0.2 and α=-1

This parameter decreases near the hot wall and by approaching to the permeable wall, the amount of microrotation increases.

Also, this parameter is positive near the hot wall and will be negative by closing to the permeable wall. With respect to the considered boundary conditions, for the microrotation parameter in this problem (S=0) the micro rotation value near the walls is zero.

The effect of expanding ratio (α) on velocity components are indicated in Figure 7 for φ=0.02, q=0.2, Re=1. $\alpha > 0$ shows expanding and $\alpha < 0$ indicates contracting. The axial velocity component increases with an increase of α, although the normal velocity component increases up to a distinctive η for each α and then decreases.

In fact, it can be said that the normal velocity has the critical point that by expanding the walls of the channel, it increases and approaches to the hot wall.

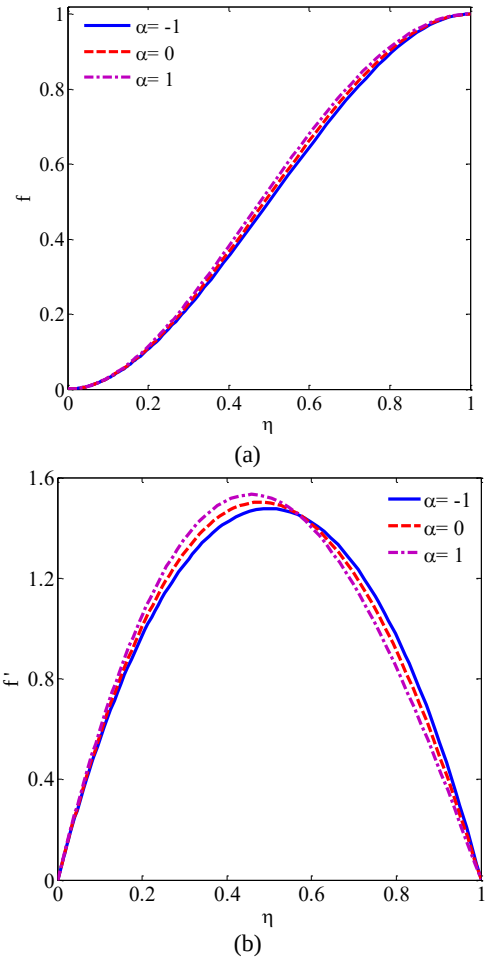

Fig. 7. Effect of expanding ratio on (a). f and (b). f' for φ=0.02, q=0.2 and Re=1

Figure 8 represents the behaviour of the hybrid nanofluid temperature when α increases. As expected, by expanding the distance between two walls of channel, the temperature of hybrid nanofluid between two plates increases.

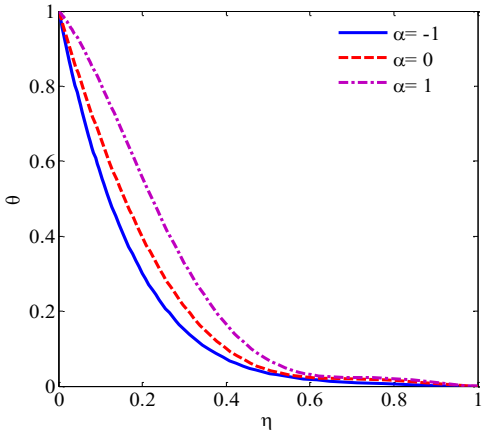

Fig. 8. Effect of expanding ratio on θ when for φ=0.02, q=0.2 and Re=1

Figure 9 shows the effect of α on the variations of hybrid nanofluid microrotation in terms of η. These variations

have two critical points in the distance between two walls of channel. By increasing α, the microrotation near the hot wall and permeable wall decreases and increases, respectively. g near the center of the channel has inflection point and its value in this point is zero. In addition, by increasing α, this point is closed to the hot wall.

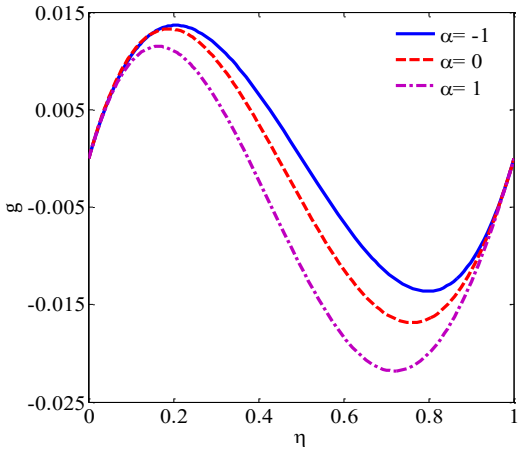

Fig. 9. Effect of expanding ratio on g when for φ=0.02, q=0.2 and Re=1

In Figures 10 and 11, the effect of q on velocity components and temperature of hybrid nanofluid are investigated.

This parameter does not have significant impact on the velocity and temperature components. When q increases the axial velocity close to the hot wall decreases slightly and the normal velocity has the maximum value in the center of the channel. As can be seen in Figure 12, the increment of q causes an increase in g and the discrepancy between the maximum and minimum values of the micro rotation. In different values of q, the curve of g still has three points that are zero that shows in addition to the top and bottom walls which have the zero microrotation, in the center of the channel this characteristic is zero too.

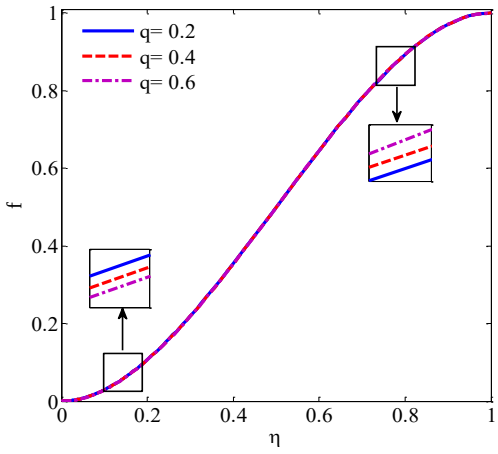

(a)

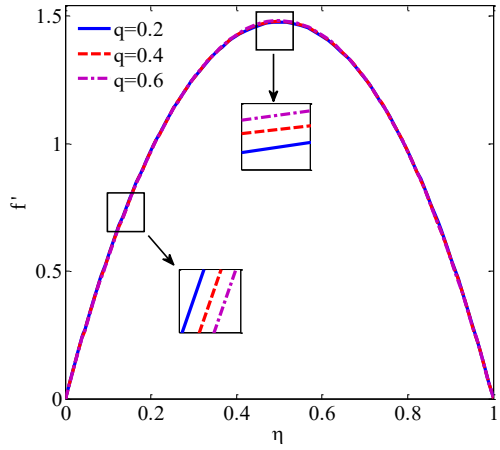

(b)

Fig. 10. Effect of q on (a). f and (b). f' for φ=0.02, Re=1 and α=-1.

The influence of the volume fraction of nanoparticles on axial and normal velocity profiles are illustrated in Figure 13.

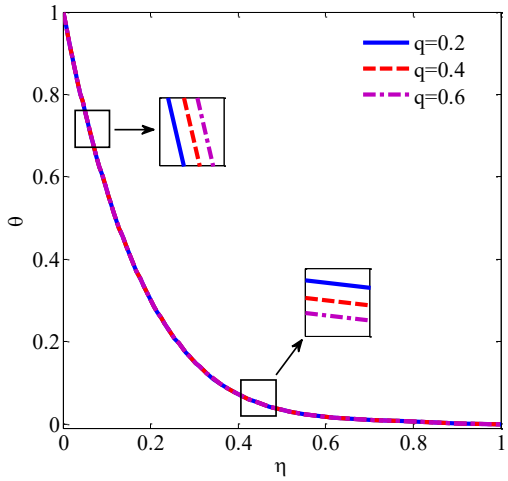

Fig. 11. Effect of q on θ when φ=0.02, Re=1 and α=-1

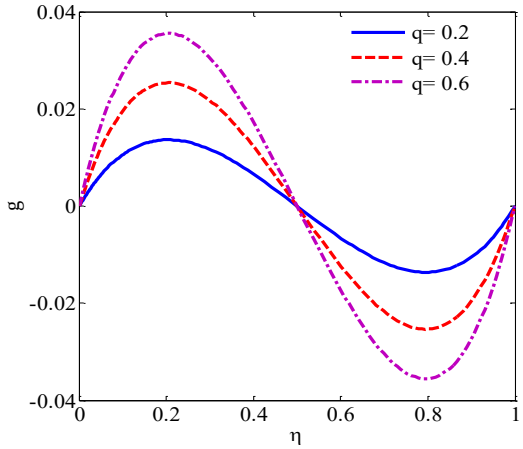

Fig. 12. Effect of q on g when φ=0.02, Re=1 and α=-1

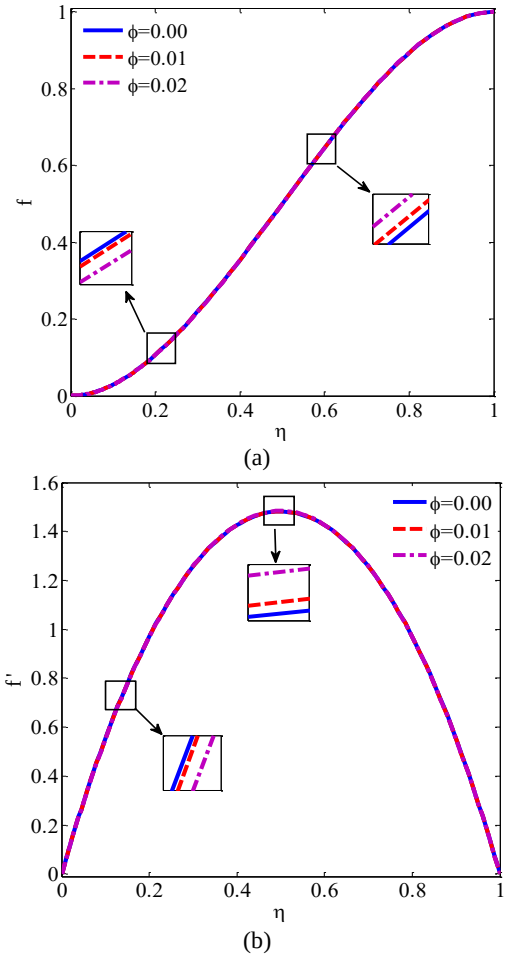

Fig. 13. Effect of volume fraction of nanoparticles on (a). f and (b). f' for q=0.2, Re=1 and α=-1

The axial velocity component decreases near the hot wall by increasing the volume fraction of nanoparticles, while the normal velocity components near the two walls decrease and in the area between two walls increase. Figure 14 shows that by increasing the volume fraction of nanoparticles, the temperature of the hybrid nanofluid increases.

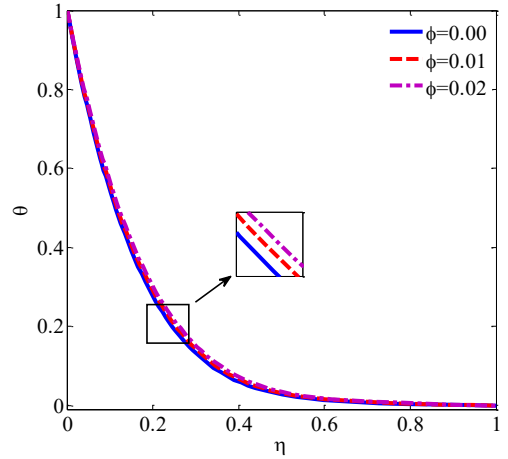

Fig. 14. Effect of volume fraction on θ when q=0.2, Re=1 and α=-1

The impact of the volume fraction of nanoparticles on microrotation of hybrid nanofluid is shown in Figure 15. It is obvious that when the volume fraction of nanoparticles increases, the value of g decreases but the critical point and inflection points in the curve are remained fixed.

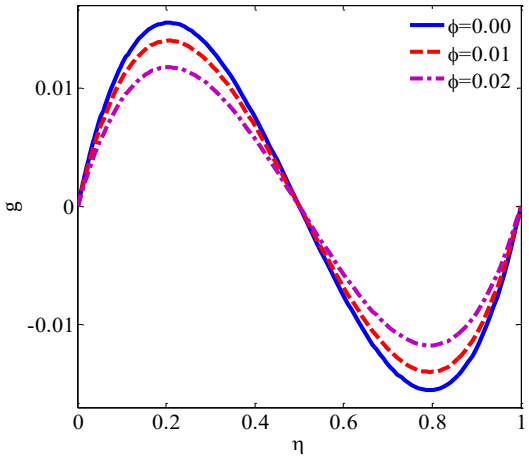

Fig. 15. Effect of volume fraction on g when q=0.2, Re=1 and α=-1

Comparison of the flow field and heat transfer between the nanofluid and hybrid nanofluid

By considering the definition for the Nusselt number in equation 24, Figure 16 indicates that the Nusselt number increases by increasing the volume fraction of nanoparticles and Reynolds number. Since adding the nanoparticles increases the coefficient of equivalent thermal conductivity, but locally the synthesis of this effects increases the Nusselt number.

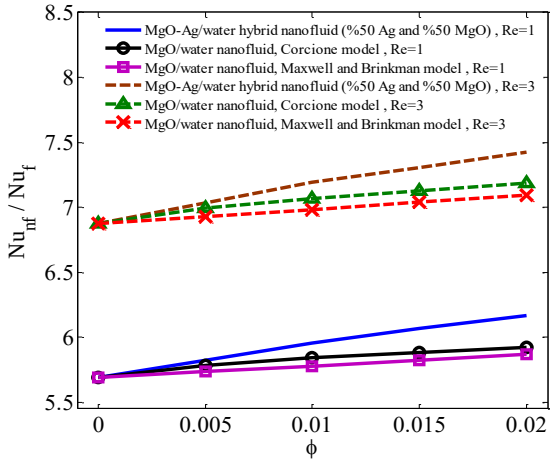

Fig. 16. Comparison between the results of using MgO nanoparticles and hybrid of MgO- Ag nanoparticles on Nu when φ=0.02, q=0.2 and α=-1

Also the results of using MgO nanoparticles compared with hybrid of MgO-Ag nanoparticles shows that using of the hybrid of nanoparticles has a striking influence on increment of heat transfer. Also, In order to calculate the thermal conductivity coefficient and viscosity of

MgO/water nanofluid, one time the relation 5 and 6 has been employed and another time, the relations 7 and 8 has been used. According to Figure 16, when the hybrid nanofluid is used, the Nusselt number is more than when the MgO is used. In addition, the Nusselt number is high when the Corsine relations are employed compared to when Maxwell and Brinkman relations.

Figure 17 also illustrates the effect of using hybrid nanofluid on velocity components. As can be seen, in high Reynolds number, the difference between two models is perceptible and applying the hybrid nanofluid causes in increasing the axial velocity in the area between two walls and the normal velocity near the hot wall. In Figure 18, the effect of using hybrid nanoparticles on temperature is studied. Using the hybrid nanoparticles increases the temperature.

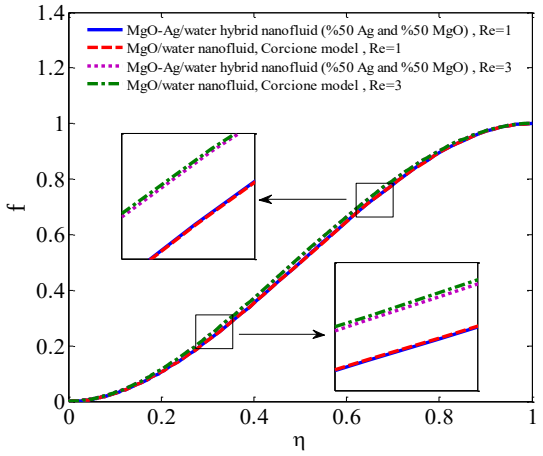

(a)

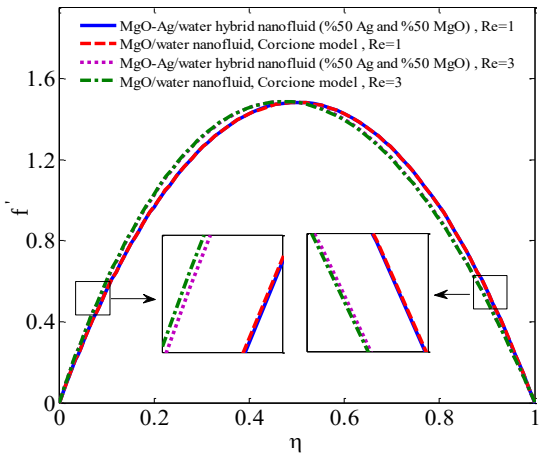

(b)

Fig. 17. Comparison between the results of using MgO nanoparticles and hybrid of MgO- Ag nanoparticles on (a). f and (b). f' for φ=0.02, q=0.2 and α=-1

In Figure 19, the effect of hybrid nanoparticles on micro rotation of micropolar fluid is examined. Using the hybrid nanoparticles decreases the microrotation near the two walls.

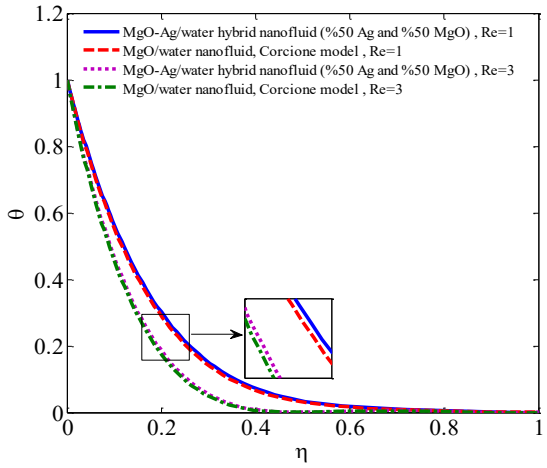

Fig. 18. Comparison between the results of using MgO nanoparticles and hybrid of MgO- Ag nanoparticles on θ when φ=0.02, q=0.2 and α=-1

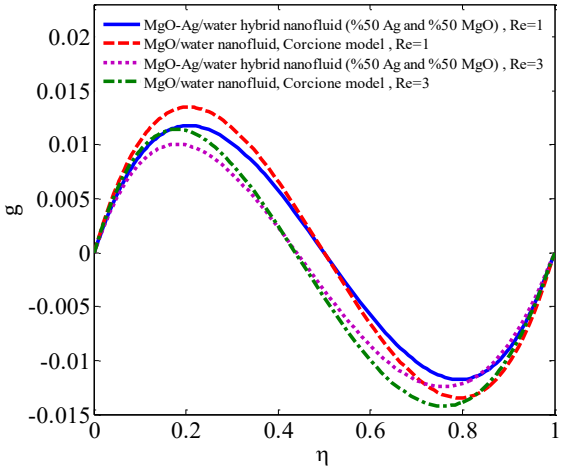

Fig. 19. Comparison between the results of using MgO nanoparticles and hybrid of MgO-Ag nanoparticles on g when φ=0.02, q=0.2 and α=-1

CONCLUSION

In this study, the effect of using the micropolar hybrid nanofluid in a permeable channel with expanding and contracting walls are studied by using LSM analytical method and fourth order Rung-Kutta numerical method. The comparison between the analytical and numerical method represents the high accuracy of the analytical method which is applied to solve the non-linear system of equations in a specified range. According to the obtained results it is obvious that:

1. By increasing the Reynolds number, the axial velocity components increase in the area between the two walls; while the normal velocity components near the hot wall increase and near the permeable wall decrease.
2. By increasing the Reynolds number, the temperature of the nanofluid reduces in the area between the two walls; while the microrotation

parameters near the hot wall decrease and near the porous wall increase.

3. The axial velocity components and the nanofluid temperature increase when α increases but the normal velocity components increase up to the specified η and then decrease. The value of microrotation parameters near the hot wall reduce and near the porous wall increase.
4. Using nanoparticles changes the velocity components slightly but increases the temperature of the nanofluid and decreases microrotation.
5. Applying hybrid nanofluid enhances heat transfer especially in high Reynolds and volume fraction of nanoparticles.

6. Acknowledgment

The authors wish to thank the Energy Research Institute of the University of Kashan for their support regarding this research (grant no. 65473).

REFERENCES

[1] Choi SU, Eastman JA. Enhancing thermal conductivity of fluids with nanoparticles. Argonne National Lab., IL (United States); 1995 Oct 1.

[2] Khanafer K, Vafai K, Lightstone M. Buoyancy-driven heat transfer enhancement in a two-dimensional enclosure utilizing nanofluids. International journal of heat and mass transfer. 2003 Sep 30;46(19):3639-53.

[3] Roy G, Nguyen CT, Lajoie PR. Numerical investigation of laminar flow and heat transfer in a radial flow cooling system with the use of nanofluids. Superlattices and Microstructures. 2004 Jun 30;35(3):497-511.

[4] Maiga SE, Palm SJ, Nguyen CT, Roy G, Galanis N. Heat transfer enhancement by using nanofluids in forced convection flows. International journal of heat and fluid flow. 2005 Aug 31;26(4):530-46.

[5] Ho CJ, Chen MW, Li ZW. Numerical simulation of natural convection of nanofluid in a square enclosure: effects due to uncertainties of viscosity and thermal conductivity. International Journal of Heat and Mass Transfer. 2008 Aug 31;51(17):4506-16.

[6] Yang YT, Lai FH. Numerical study of heat transfer enhancement with the use of nanofluids in radial flow cooling system. International Journal of Heat and Mass Transfer. 2010 Dec 31;53(25):5895-904.

[7] Sheikhzadeh GA, Arefmanesh A, Kheirkhah MH, Abdollahi R. Natural convection of Cu–water nanofluid in a cavity with partially active side walls. European Journal of Mechanics-B/Fluids. 2011 Apr 30;30(2):166-76.

[8] Ahmed MA, Shuaib NH, Yusoff MZ. Numerical investigations on the heat transfer enhancement in a wavy channel using nanofluid. International Journal of Heat and Mass Transfer. 2012 Oct 31;55(21):5891-8.

[9] Abbasi FM, Hayat T, Ahmad B. Peristalsis of silver-water nanofluid in the presence of Hall and Ohmic heating effects: applications in drug delivery. Journal of Molecular Liquids. 2015 Jul 31;207:248-55.

[10] Sheikholeslami M, Hatami M, Ganji DD. Numerical investigation of nanofluid spraying on an inclined rotating disk for cooling process. Journal of Molecular Liquids. 2015 Nov 30;211:577-83.

[11] Sheikholeslami M, Rashidi MM, Ganji DD. Numerical investigation of magnetic nanofluid forced convective heat transfer in existence of variable magnetic field using two phase model. Journal of Molecular Liquids. 2015 Dec 31;212:117-26.

[12] Zhao N, Yang J, Li H, Zhang Z, Li S. Numerical investigations of laminar heat transfer and flow performance of Al_2O_3–water nanofluids in a flat tube. International Journal of Heat and Mass Transfer. 2016 Jan 31;92:268-82.

[13] Bianco V, Chiacchio F, Manca O, Nardini S. Numerical investigation of nanofluids forced convection in circular tubes. Applied Thermal Engineering. 2009 Dec 31;29(17):3632-42.

[14] Tahir S, Mital M. Numerical investigation of laminar nanofluid developing flow and heat transfer in a circular channel. Applied Thermal Engineering. 2012 Jun 30;39:8-14.

[15] Sheikholeslami M, Ganji DD, Rokni HB. Nanofluid flow in a semi-porous channel in the presence of uniform magnetic field. International Journal of Engineering-Transactions C: Aspects. 2013 Jan 24;26(6):653.

[16] Wang X, Xu X, Choi SU. Thermal conductivity of nanoparticle-fluid mixture. Journal of thermophysics and heat transfer. 1999 Oct 1;13(4):474-80.

[17] Selvakumar P, Suresh S. Use of Al_2O_3–Cu/water hybrid nanofluid in an electronic heat sink. IEEE Transactions on Components, Packaging and Manufacturing Technology. 2012 Oct;2(10):1600-7.

[18] Suresh S, Venkitaraj KP, Selvakumar P, Chandrasekar M. Effect of Al_2O_3–Cu/water hybrid nanofluid in heat transfer. Experimental Thermal and Fluid Science. 2012 Apr 30;38:54-60.

[19] Esfe MH, Arani AA, Rezaie M, Yan WM, Karimipour A. Experimental determination of thermal conductivity and dynamic viscosity of Ag–MgO/water hybrid nanofluid. International

Communications in Heat and Mass Transfer. 2015 Aug 31;66:189-95.

[20] Moghadassi A, Ghomi E, Parvizian F. A numerical study of water based Al_2O_3 and Al_2O_3–Cu hybrid nanofluid effect on forced convective heat transfer. International Journal of Thermal Sciences. 2015 Jun 30;92:50-7.

[21] Eringen AC. Theory of micropolar fluids. Journal of Mathematics and Mechanics. 1966 Jul 1:1-8.

[22] Bourantas GC, Loukopoulos VC. Modeling the natural convective flow of micropolar nanofluids. International Journal of Heat and Mass Transfer. 2014 Jan 31;68:35-41.

[23] Hussain ST, Nadeem S, Haq RU. Model-based analysis of micropolar nanofluid flow over a stretching surface. The European Physical Journal Plus. 2014 Aug 1;129(8):161.

[24] Ahmed SE, Mansour MA, Hussein AK, Sivasankaran S. Mixed convection from a discrete heat source in enclosures with two adjacent moving walls and filled with micropolar nanofluids. Engineering Science and Technology, an International Journal. 2016 Mar 31;19(1):364-76.

[25] Sheikholeslami M, Hatami M, Ganji DD. Micropolar fluid flow and heat transfer in a permeable channel using analytical method. Journal of Molecular Liquids. 2014 Jun 30;194:30-6.

[26] Bourantas GC, Loukopoulos VC. MHD natural-convection flow in an inclined square enclosure filled with a micropolar-nanofluid. International Journal of Heat and Mass Transfer. 2014 Dec 31;79:930-44.

[27] Turkyilmazoglu M. A note on micropolar fluid flow and heat transfer over a porous shrinking sheet. International Journal of Heat and Mass Transfer. 2014 May 31;72:388-91.

[28] Jena SK, Malla LK, Mahapatra SK, Chamkha AJ. Transient buoyancy-opposed double diffusive convection of micropolar fluids in a square enclosure. International Journal of Heat and Mass Transfer. 2015 Feb 28;81:681-94.

[29] Fakour M, Vahabzadeh A, Ganji DD, Hatami M. Analytical study of micropolar fluid flow and heat transfer in a channel with permeable walls. Journal of Molecular Liquids. 2015 Apr 30;204:198-204.

[30] Borrelli A, Giantesio G, Patria MC. Magnetoconvection of a micropolar fluid in a vertical channel. International Journal of Heat and Mass Transfer. 2015 Jan 31;80:614-25.

[31] Stern RH, Rasmussen H. Left ventricular ejection: model solution by collocation, an approximate analytical method. Computers in biology and medicine. 1996 May 1;26(3):255-61.

[32] Vaferi B, Salimi V, Baniani DD, Jahanmiri A, Khedri S. Prediction of transient pressure response in the petroleum reservoirs using orthogonal collocation. Journal of Petroleum Science and Engineering. 2012 Nov 30;98:156-63.

[33] Aziz A, Bouaziz MN. A least squares method for a longitudinal fin with temperature dependent internal heat generation and thermal conductivity. Energy conversion and Management. 2011 Aug 31;52(8):2876-82.

[34] Sheikholeslami M, Hatami M, Ganji DD. Analytical investigation of MHD nanofluid flow in a semi-porous channel. Powder Technology. 2013 Sep 30;246:327-36.

[35] Hatami M, Sheikholeslami M, Ganji DD. Nanofluid flow and heat transfer in an asymmetric porous channel with expanding or contracting wall. Journal of Molecular Liquids. 2014 Jul 31;195:230-9.

[36] Hatami M, Sheikholeslami M, Ganji DD. Laminar flow and heat transfer of nanofluid between contracting and rotating disks by least square method. Powder Technology. 2014 Feb 28;253:769-79.

[37] Davarnejad R, Jamshidzadeh M. CFD modeling of heat transfer performance of MgO-water nanofluid under turbulent flow. Engineering Science and Technology, an International Journal. 2015 Dec 31;18(4):536-42.

[38] Das SK, Choi SU, Yu W, Pradeep T. Nanofluids: science and technology. John Wiley & Sons; 2007 Dec 4.

[39] Xuan Y, Roetzel W. Conceptions for heat transfer correlation of nanofluids. International Journal of heat and Mass transfer. 2000 Oct 1;43(19):3701-7.

[40] Labib MN, Nine MJ, Afrianto H, Chung H, Jeong H. Numerical investigation on effect of base fluids and hybrid nanofluid in forced convective heat transfer. International Journal of Thermal Sciences. 2013 Sep 30;71:163-71.

[41] Nimmagadda R, Venkatasubbaiah K. Conjugate heat transfer analysis of micro-channel using novel hybrid nanofluids (). European Journal of Mechanics-B/Fluids. 2015 Aug 31;52:19-27.

[42] Devi SS, Devi SA. Numerical investigation of three-dimensional hybrid Cu–Al_2O_3/water nanofluid flow over a stretching sheet with effecting Lorentz force subject to Newtonian heating. Canadian Journal of Physics. 2016 Mar 2;94(5):490-6.

[43] Balla HH, Abdullah S, MohdFaizal W, Zulkifli R, Sopian K. Numerical study of the enhancement of heat transfer for hybrid CuO-Cu nanofluids flowing in a circular pipe. Journal of oleo science. 2013;62(7):533-9.

[44] Maxwell JC. A treatise on electricity and magnetism. Clarendon press; 1881.

[45] Brinkman HC. The viscosity of concentrated suspensions and solutions. The Journal of Chemical Physics. 1952 Apr;20(4):571-.

[46] Corcione M. Empirical correlating equations for predicting the effective thermal conductivity and

dynamic viscosity of nanofluids. Energy Conversion and Management. 2011 Jan 31;52(1):789-93.

[47] Sibanda P, Awad F. Flow of a micropolar fluid in channel with heat and mass transfer. Fluid Mechanics and Heat & Mass Transfer. 2010 Jul 22.

[48] Aziz A. Heat conduction with maple, RT Edwards. Inc., Philadelphia. 2006.